

Model reduction in the physical domain

A Y Orbak¹, O S Turkay^{2*.*.*}, E Eskinat¹ and K Youcef-Toumi³

¹Department of Industrial Engineering, Uludag University, Bursa, Turkey

²Department of Mechanical Engineering, Yeditepe University, Istanbul, Turkey

³Department of Mechanical Engineering, Massachusetts Institute of Technology, Cambridge, Massachusetts, USA

Abstract: This paper is concerned with obtaining physical-based low-order approximations of linear physical systems. Low-order models possess some advantages, including the reduction of computational difficulty and understanding of the physics of the original system in a simpler manner. Previously, a number of methods have been suggested to develop suitable low-order approximations. However, most of these approaches do not reflect the relation between the mathematical model and the physical subsystems. Specifically, these techniques do not indicate which of the physical subsystems should be retained or eliminated in the reduced-order model. The proposed model reduction method is based on identifying subsystem types of a physical system using the bond graph method. These subsystems are then removed or retained based on the information from the physical system decomposition procedures and partial fraction expansion residues to obtain a reduced-order model. The physical model reduction procedure is verified on physical linear systems.

Keywords: model reduction, bond graphs, physical systems

NOTATION

A, B, C, D	system matrices
b	damper coefficient (N s/m)
C	bond graph capacitance element
F	force input (N)
F_{k_i}	force in spring i (N)
G_{IC}	I - C loop gain
G_{IR}	sum of loop gains of I - R pairs
G_{RC}	sum of loop gains of R - C pairs
l	bond graph inertial element
k	spring coefficient (N/m)
m	mass (kg)
R	bond graph resistance element
u	input vector
x	state vector
y	output vector
ζ_{i-j}	local damping ratio of the local loop between mass i and mass j
λ	eigenvalue
ω	frequency (rad/s)

0	bond graph common effort junction
1	bond graph common flow junction

1 INTRODUCTION

For complex dynamic systems it is often useful to find a simplified model for purposes such as controller design, parameter optimization, design assessment under uncertainty and to obtain a better insight into the system behaviour. Consequently, the model reduction methods have been investigated in control system analysis for many years and several methods have been suggested for determining low-order approximations. Model reduction techniques serve two important tasks in solving control engineering problems. Firstly, a model order reduction is effective to render control design problems to a manageable size when using modern control synthesis methods. Secondly, the controller order reduction is an interesting research area that enables simpler hardware/software controllers to be obtained.

It is frequently desired to approximate a high-order model by a reduced-order model in such a way that the relevant dynamics is preserved in the low-order model. Mathematically, this is usually carried out by minimization of a suitable error norm. Most of the techniques in the literature take into account a criterion for the 'goodness' of the reduced model. For example, the balancing approach [1] uses coordinate transformations to

The MS was received on 16 May 2003 and was accepted after revision for publication on 6 October 2003.

* Corresponding author: Department of Mechanical Engineering, Faculty of Engineering and Architecture, Yeditepe University, K. Bakkalkoy/Kadikoy-81120, Istanbul, Turkey.

** Formerly at Department of Mechanical Engineering, Bogazici University, Istanbul, Turkey.

convert the system to a special balanced form from which a reduced model can be obtained. The techniques based on balancing aim to reduce the order of the transfer matrix between the input and output by targeting worst-case scenarios. Therefore, the error bound of the reduced model is guaranteed. However, transfer matrices and their realizations do not contain the information about the internal structure of the system. Therefore, in general, these procedures may not be directly applied to the modelling and reduction of physical systems.

Several time and frequency domain methods exist that generally provide good approximations. Some of the well-known time domain methods are the approximate moment matching method [2], which utilizes the elimination of some time moments with the employment of a singular-value decomposition approximation, and the least-squares model reduction method [3], which uses the power of curve-fitting by calculating a low-order autoregressive moving average (ARMA) predictor equation. A number of the principal frequency domain methods are the following: the component cost analysis for model reduction [4], which uses a quadratic cost measure for eliminating the modes, Padé approximations [5] and continued fraction methods [6], which employ the continued fraction expansion and inversion processes with a generalized matrix Routh algorithm to expand a matrix transfer function into the matrix continued fraction of matrix Caue forms. Additionally, balance and truncate types of approaches [7], which exploit the balancing idea, are present in which the drawbacks of reference [1] are eliminated via projections defined in terms of arbitrary bases for the left and right eigenspaces associated with the large eigenvalues of the product of the observability and controllability gramians.

In addition to the above approaches, active researches of model reduction in the physical domain based on power criteria are being conducted. In these methods either the components associated with small power flow are eliminated, as they have only a small contribution to the dynamic behaviour of a system [8, 9], or a singular perturbation method is used to reduce the dimension of the system by considering only one part, namely the slow or fast part, depending on the frequency domain of interest [10].

The power method uses various time averages of the power flow associated with a component to measure the corresponding power level [8] or energy level [9]. The model reduction approaches in references [8] and [9] are conceptually similar to each other. These are established on power/energy criteria and consist of the following three major steps: (a) calculating the system's time response under certain inputs with numerical simulation, (b) measuring the power flow in and out of a component and (c) removing the components associated with a low-power flow level. Specifically, Rosenberg and Zhou [8] used bond graphs for measuring the power response to determine a simplified model for controller design and

parameter optimization and to gain insight into the model behaviour. The power responses are obtained by applying a step input for a given time interval and calculating the power on all bonds of the bond graph. Then, a root mean square (r.m.s.) average of each power is calculated. Finally, the bonds with low average values are eliminated from the bond graph model. Louca *et al.* [9] preferred to employ energy as a metric instead of power because as energy is the time integral of power it is more advantageous to use it throughout the simulation time in case there are time-varying elements in the system. The authors claimed that the r.m.s. power metric might also provide false information due to heavy weighing of peak responses. Hence they defined an energy-based 'element activity index', which is calculated as the ratio of the energy flowing through an element to the total system energy. Then the bonds that are deemed unnecessary are eliminated from the bond graph model by removing the low activity elements to a chosen appropriate threshold value. The attractive advantage of the method is that by utilizing the sinusoidal excitation input the most appropriate reduced model can be obtained as a function of a predefined frequency range of interest. Although the authors claimed that the method could be applied for model reduction of non-linear systems, they acknowledged the need for further study of the application of the method to non-linear models. The methods [8, 9] are not strictly proven mathematically, but they have of course clear physical interpretations for model reduction. They eliminate elements that are considered unnecessary according to power or energy level information without indicating which subsystems to retain or remove in a systemic perspective view, which is the method explained in this paper.

Another physical-based model reduction technique developed by Sueur and Dauphin-Tanguy [10] makes use of the singular perturbation method. The fast and slow dynamics of bond graph models are estimated by determination of causal loop gains and by utilizing reciprocal systems. In this method, when the dynamic subsystems are well separated, the resulting reduced model is very near to the one deduced from the singular perturbation method.

In this paper, a physical-based model reduction procedure is developed and assessed. The method leads to an appropriate reduced-order model while retaining a physical relevance to the full-order model. The proposed methodology exploits the concept of decomposition of physical systems suitable for identification of dominant subsystems. For this purpose the idea of Sueur and Dauphin-Tanguy [10] is developed for more general systems. Using the extended decomposition procedures, different types of behaviour of a dynamic system are identified. The dynamic behaviours of a system are classified in three main categories: (a) fast-slow dynamics as in reference [10], (b) high-low-frequency oscillation modes and (c) heavily-lightly damped dynamics.

The use of type (b) and type (c) dynamics in conjunction with the residues and eigenvalues information for model reduction constitutes the main contribution of the present method. The decomposition and model reduction procedures are implemented on the model directly, providing a better perception of the physical model reduction and a better design point of view [11]. This method is more suitable for weakly coupled systems from an application point of view.

In section 2, the information for the decomposition procedures are given and the method of physical model reduction is explained. In section 3 a few examples are considered to show the implementation of model reduction for the assessment of the proposed method and its results.

2 PHYSICAL DOMAIN MODEL REDUCTION

As mentioned in the previous section, the decomposition procedures are used to identify fast–slow dynamics, high–low frequency oscillation modes and heavily–lightly damped dynamic subsystems for the purpose of physical model reduction. Then these subsystems are associated with the partial fraction expansion residues and eigenvalues of the system. As a last step, the relevant physical subsystems are retained by considering the absolute values of the residues (the norm in the multi-input, multi-output case) of the full model for obtaining a reduced-order model.

The identification of three principal types of dynamic behaviour in a linear system will be explored in section 2.1. Then in section 2.2 the physical model reduction procedure will be explained.

2.1 Identification of various dynamic behaviours of linear systems

The system structure information is obtained by carrying out the decompositions in the physical domain. These decompositions are utilized to identify the subsystems that are responsible for the different dynamic characteristics of the system, such as fast and slow dynamics, high- and low-frequency oscillation modes and heavily and lightly damped dynamics. The procedure is performed directly on the system using the bond graph models that describe the dynamic behaviour of the physical system by the connection of lumped and idealized elements based on the conservation of energy principle. In the next subsections these decomposition procedures will be explained in detail.

2.1.1 Decomposition of fast and slow dynamics

When a system contains fast and slow dynamics, it is well known that the slow dynamics dominate the system behaviour. Therefore, the eigenvalues corresponding to

the fast dynamics can safely be ignored in the analysis. In case the system contains only resistance R and inertance I elements, or R and capacitance C elements, all of the eigenvalues of the system will always be real. Thus, the elements that are involved with fast or slow dynamics can be identified as in reference [10]; i.e. the system can be decomposed into two timescales. This identification is carried out using reciprocal bond graphs and by decomposing the system into fast reduced and slow reduced bond graphs using the local loop gain concept. Local loops are the loops between the physical components of a bond graph that have a causal relationship.

As an example, consider a simple R – C circuit and its corresponding bond graph model, as shown in Fig. 1. In this model, the capacitance element C_1 imposes effort to the 0-junction, then through the 1-junction to the resistance element R_1 . The element R_1 imposes a flow to the 1-junction and through the 0-junction to the element C_1 . Therefore, a causal loop is formed between these two elements. Local loop gains are calculated as follows. For an I – R loop the loop gain is equal to R/I , for an R – C loop the loop gain is equal to $1/(RC)$ and for an I – C loop the loop gain is equal to $1/(IC)$. The I – R or R – C loop gains represent the energy dissipation rates in the local loops for the corresponding energy storage elements. On the other hand, the square roots of the I – C loop gains represent the energy exchange rates in the local loops. Thus, the loop gain of the above causal path is computed as $1/(R_1 C_1)$. Similarly, a causal loop is formed between the elements R_1 and C_2 , C_2 and R_2 , R_2 and C_3 , and C_3 and R_3 .

Now, the information for the two timescales can be extracted as follows. Suppose that the element C_2 has a particularly small value; then the loop gain $1/(R_1 C_2)$ and $1/(R_2 C_2)$ will become much larger than the others. This means that the energy stored in the capacitance C_2 will be dissipated by R_1 and R_2 very quickly. Therefore, the elements R_1 , C_2 and R_2 together with the junctions that the causal loops pass through represent the fast dynamics, as shown in Fig. 2a. Once the fast dynamics reaches its equilibrium status, $\dot{q}_2 = 0$, the element C_2 plays no role in the slow dynamics. Replacing the element C_2 with a flow source of zero value can realize this condition.

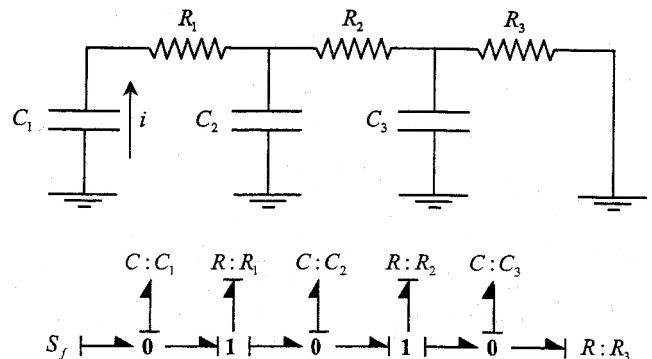


Fig. 1 An R – C system and its corresponding bond graph

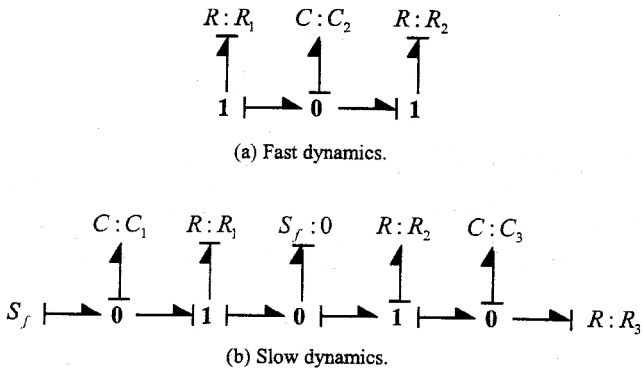


Fig. 2 The bond graph model of the fast and slow dynamics

Thus, the model shown in Fig. 2b represents the slow dynamics. It is important to note that, if the equations are derived according to the models in Fig. 2, they will be exactly the same as those derived using the perturbation theory. With this approach, the physical elements and the system structures that are responsible for the fast or slow dynamics can be clearly identified.

2.1.2 Decomposition of high- and low-frequency oscillation modes

If a system contains only energy storage elements, i.e. inertial I and capacitance C elements, all of the eigenvalues of the system will be on the imaginary axis and the system will exhibit pure oscillations. In this case as an $I-C$ network can be transformed into a fictitious $R-C$ or $R-I$ network [12], the decomposition explained to obtain fast and slow dynamics could be extended to $I-C$ systems without any modification. Thus, the subsystems that are responsible for the high- and low-frequency oscillation modes can be identified if the system contains well-separated eigenvalues. As an example, consider the simple cascaded mass-spring system shown in Fig. 3. Two cases may be examined. In the first case, suppose that the element C_2 has a much smaller value, i.e. this spring is much stiffer than the other two springs, which have the same order of magnitude. By examining the local loop gains, it can be observed that the loop gain associated with elements C_2, I_1 (k_2/m_1), and the one associated with C_2, I_2 (k_2/m_2) are much larger than the others ($k_1/m_1, k_3/m_2, k_3/m_3$). The decomposition procedure indicates that the subsystems shown in Figs 4a

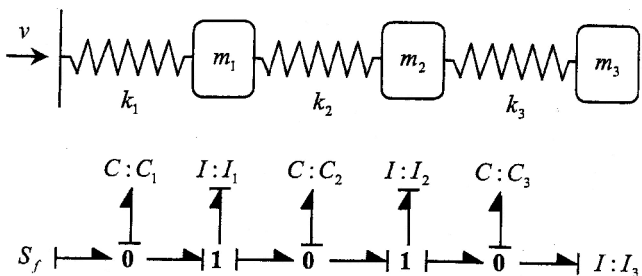


Fig. 3 An $I-C$ system and its corresponding bond graph

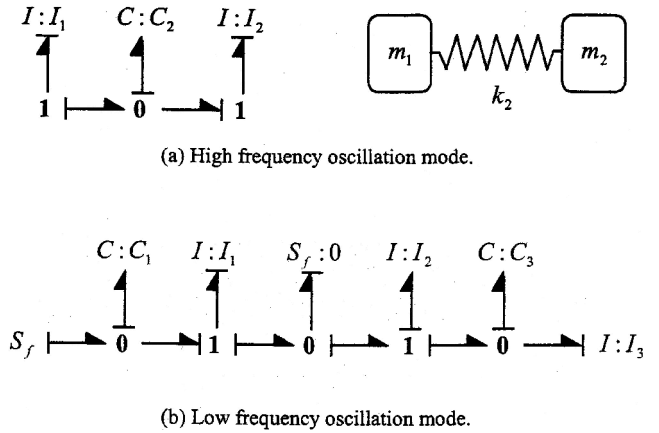


Fig. 4 High- and low-frequency oscillation modes (case 1)

and b represent the high-frequency oscillation mode and the low-frequency oscillation mode respectively. In the low-frequency oscillation mode, since the elements I_1 and I_2 are causally connected directly, these elements can be grouped and represented by an equivalent I element as shown in Fig. 5. The physical interpretation of this decomposition is that in the high-frequency oscillation mode, the soft springs have only minor effects on the system behaviour. Therefore, they do not appear in the model. However, the stiff spring behaves like a rigid link in the low-frequency oscillation mode. The effects of elements I_1 and I_2 are therefore difficult to distinguish. As a second case, assume that the mass m_2 has a much smaller value than the other two masses, which have the same order of magnitude. In this case, since the loop gains k_1/m_2 and k_2/m_2 are much smaller than $k_1/m_1, k_2/m_3$ and k_3/m_3 , the subsystem representing the high-frequency oscillation mode will be as shown in Fig. 6a. Consequently, the subsystem representing the low-frequency oscillation mode is formed by replacing I_2 with an effort source of 0 value, as shown in Fig. 6b. In this subsystem, the elements C_2 and C_3 are causally connected directly. Therefore, they can be grouped into an equivalent C element, as shown in Fig. 7. The physical interpretation of this decomposition is that in the high-frequency oscillation mode, the large inertance elements behave like rigid boundaries. On the other hand, the small mass has almost no effect on the dynamics in the

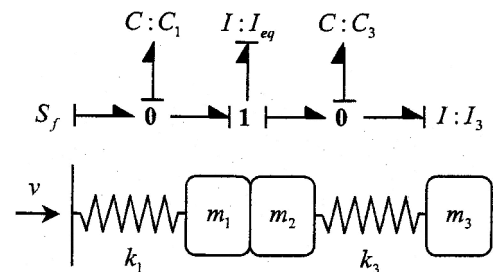


Fig. 5 Equivalent representation of the low-frequency oscillation mode (case 1)

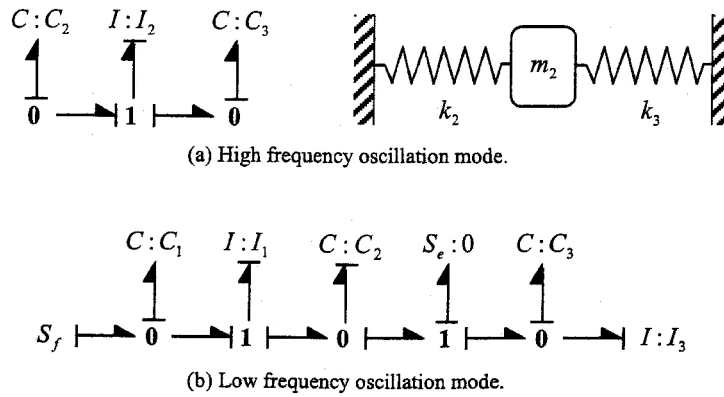


Fig. 6 High- and low-frequency oscillation modes (case 2)

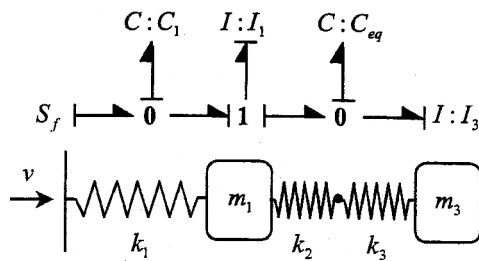


Fig. 7 Equivalent representation of the low-frequency oscillation mode (case 2)

low-frequency oscillation mode. Thus, it does not appear in the model.

2.1.3 Decomposition of lightly and heavily damped subsystems

When the system has R , C and I elements at the same time, an additional dynamic behaviour that needs to be identified is the heavily damped and lightly damped modes. In order to identify them, the procedures explained before should be extended to this more general case. For this purpose an improved procedure described below can be applied. For this identification, in addition to the loop gains for each energy storage element, the local damping ratios should also be calculated. For each directly causally related I - C pair in the system (with R elements causally connected to either I or C or both elements), the local damping ratios are calculated as $G_{RC}/(2\sqrt{G_{IC}})$ and $G_{IR}/(2\sqrt{G_{IC}})$ for the C and I elements respectively. In these formulae, G_{IC} represents the I - C loop gain, G_{RC} represents the sum of the loop gains of R - C pairs and G_{IR} represents the sum of the loop gains of I - R pairs. Notice that this calculation is equivalent to determining the damping ratio of a second-order system. The decomposition procedures for the identification of heavily and lightly damped subsystems are now given [11, 12].

Identification of heavily damped subsystems

1. Replace all the C elements by flow sources with 0 value and identify the remaining R - I pairs, which

are causally related directly. Denote these R - I elements and the involved junctions as part of a set called H , representing the heavily damped subsystem.

2. Restore the C elements that are replaced in the previous step. Identify the C elements, which are causally related directly to the above I elements. If $\sqrt{G_{IC}} \gg G_{IR}$, then replace the C elements by flow sources with 0 value. Denote these flow sources as part of the subsystem H . If the inequality is reversed, neglect the identified C elements.
3. Identify the I elements that become dependent due to the causalities imposed by the above sources and denote these I elements as part of the subsystem H .
4. Replace all the I elements by effort sources with 0 value and identify the remaining R - C pairs that are causally related directly. Denote the R - C elements and the involved junctions as part of the subsystem H .
5. Restore the I elements that are replaced in the previous step, identify the I elements that are causally related directly to the above C elements. If $\sqrt{G_{IC}} \gg G_{RC}$, then replace the I elements by effort sources with 0 value and denote these sources as part of the subsystem H . If the inequality is reversed, ignore the identified I elements.
6. Identify the C elements that become dependent due to the causalities imposed by the above sources; denote these C elements as part of the subsystem H .
7. Identify the resistances, which are involved in heavily damped local loops. Denote these R elements and the involved I - C pairs and junctions as part of the subsystem H .
8. Identify the C elements that are not involved in step 7, but are causally related directly to the above I elements. If $\sqrt{G_{IC}} \gg G_{IR}$, replace the C elements by flow sources with 0 value and denote these flow sources together with the involved junctions as part of the subsystem H . If the inequality is reversed, ignore the identified C elements.
9. Identify the I elements that are not involved in step 7, but are causally related directly to the above

C elements. If $\sqrt{G_{IC}} \gg G_{RC}$, replace the *I* elements by effort sources with 0 value. Denote these effort sources and the involved junctions as part of the subsystem *H*. If the inequality is reversed, ignore the identified *I* elements.

- Remove the elements that are not denoted as part of the subsystem *H*. The remaining subsystem is the heavily damped subsystem *H*.

In the above procedure, step 1 identifies the *R* and *I* elements that are responsible for the heavily damped modes, given that they affect the dynamics even if all of the capacitances are disabled. Steps 2 and 3 identify the *I* elements that are involved in the heavily damped modes by the power transmission through *I-C* loops. Steps 4 to 6 repeat the same procedure for *R-C* elements. Step 7 includes the overdamped subsystems. Steps 8 and 9 identify the *I* or *C* elements that affect the heavily damped modes by power transmission through other *I-C* loops.

Similarly, the decomposition procedure for the identification of lightly damped subsystems is explained in the following subsection [11, 12].

Identification of lightly damped subsystems

- Identify the *I-C* pairs, which are involved in lightly damped local loops. Denote these *I-C* elements as part of a set called *L*, which represents the lightly damped subsystem.
- Identify the *R* elements that are not involved in step 1 but are causally related directly to the above *I* or *C* elements. If $\sqrt{G_{IC}} \ll G_{RI}$ or $\sqrt{G_{IC}} \ll G_{RC}$, replace the resistive *R* elements by flow sources with 0 value and conductive *R* elements by effort sources with 0 value. Denote these sources as part of the subsystem *L*.
- Identify the energy storage elements that become dependent due to the causalities imposed by the above

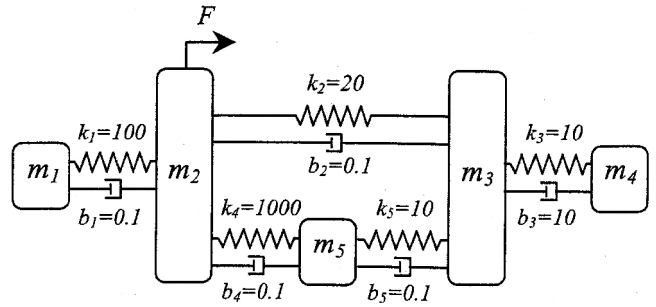


Fig. 8 A tenth-order physical system

sources. Denote these energy storage elements as part of the subsystem *L*.

- Remove the elements that are not denoted as part of the subsystem *L*. The remaining subsystem is the lightly damped subsystem *L*.

In this procedure, step 1 detects the lightly damped subsystems. Steps 2 and 3 identify the *I* or *C* elements that are involved in the lightly damped modes considering the power transmission through the other *I-R* loops. It should be noted that if multiple paths connect two elements causally then the effective loop gain is different from the sum of the loop gains corresponding to each individual path. In the latter case, the coupling between the multiple paths is not taken into account. Otherwise, the implementation of these procedures remains unchanged [12, 13].

An example on the decomposition procedure

Consider the system and its bond graph representation shown in Figs 8 and 9. There are ten independent energy storage elements in integral causality; hence, the order of the system is ten. Assume that $m_1 = m_2 = m_3 = m_4 = m_5 = 1$ kg, $k_1 = 100$ N/m, $k_2 = 20$ N/m, $k_3 = k_5 = 10$ N/m, $k_4 = 1000$ N/m, $b_1 = b_2 = b_4 = b_5 = 0.1$ N s/m

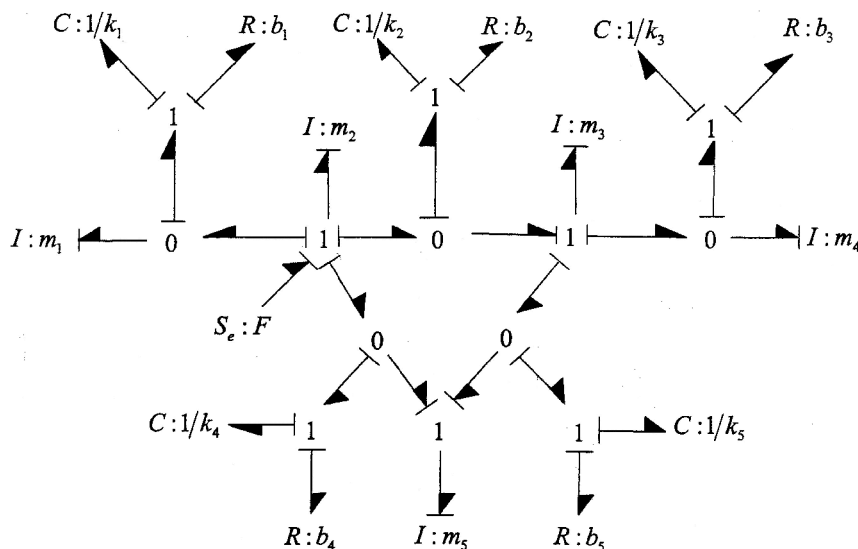


Fig. 9 Bond graph representation of the tenth-order system

and $b_3 = 10 \text{ N s/m}$. The system can be decomposed into the subsystems shown in Fig. 10, as described in the following paragraph.

It is noted that the local damping ratio $\zeta_{3,4} = b_3 / (2\sqrt{k_3 m_3}) = 1.58$ is much larger than the others [maximum $\zeta_{5,3} = b_5 / (2\sqrt{k_5 m_5}) = 0.02$ and minimum $\zeta_{2,5} = b_4 / (2\sqrt{k_4 m_5}) = 1.58 \times 10^{-3}$]. This suggests that the system can be decomposed into two subsystems representing the heavily damped modes and the lightly damped modes. The heavily damped subsystem that consists of m_3, k_3, b_3 and m_4 can further be decomposed into fast and slow dynamical subsystems, as shown in Figs 10b and d. In addition, the local loop gain $k_4/m_5 = 1000 \text{ rad/s}^2$ is much larger than the others (maximum $k_1/m_1 = k_1/m_2 = 100 \text{ rad/s}^2$, minimum $k_3/m_3 = k_3/m_4 = 10 \text{ rad/s}^2$) in the remaining lightly damped subsystem. Thus, this subsystem can be decomposed into two subsystems, as shown in Figs 10a and c, namely high-frequency and low-frequency oscillation modes. The eigenvalues of the full system and those of the subsystems are computed and tabulated in Table 1. The closeness of these values is noted, indicating the effectiveness of the decomposition technique used in the model reduction method. It is possible to quantify the

closeness by selecting a norm based on eigenvalues or on the full- and reduced-order model responses.

2.2 Physical domain model reduction procedure

Based on the decomposition procedures explained in the previous section, the proposed physical domain model reduction method consists of the following steps:

- Step 1. Obtain the linear lumped parameter model of the system and then draw the bond graph model.
- Step 2. Identify the major subsystems of the model using the decomposition procedures described above and calculate their eigenvalues.
- Step 3. It is well known from basic control theory that the residues and the eigenvalues are the parameters to assess in order to find the dominant modes of a linear system. The largest residue and the eigenvalue nearest to the imaginary axis contribute most to the dominant part of the time domain response of a linear system. Hence, in this step the eigenvalues and the partial fraction expansion residues of the full-order model are computed.
- Step 4. Match the eigenvalues that must be retained

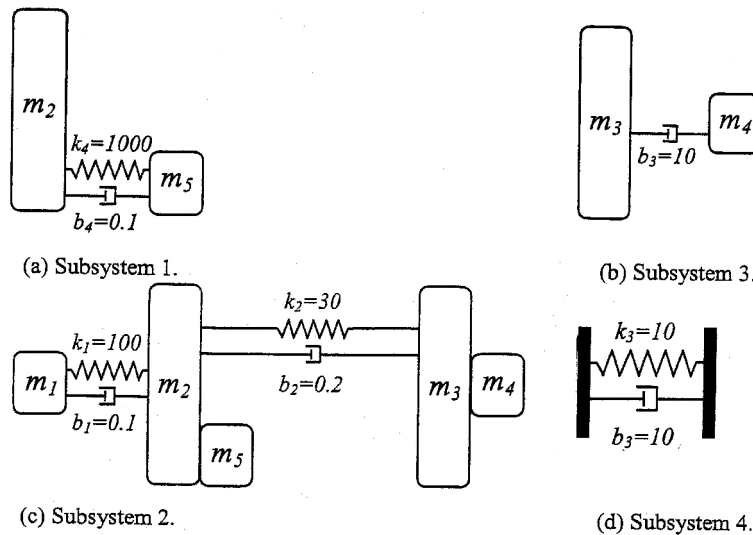


Fig. 10 Subsystems of the tenth-order system

Table 1 Eigenvalues of the original and the subsystems of the tenth-order physical system

Original system eigenvalues	Subsystem	Eigenvalues
$-0.1789 \pm 45.4882i$	1	$-0.1 \pm 44.7212i, 0$
$-0.1088 \pm 12.3218i$	2	$-0.0979 \pm 12.4875i, -0.0771 \pm 4.9031i, 0$
$-0.4498 \pm 4.8881i$	3	-20
-18.2310	4	-1
-1.0941		
0		
0		

according to step 3 together with step 2 and consequently determine the subsystems to be retained and eliminated.

In the resulting reduced-order model, there can be a d.c. gain discrepancy between the reduced- and the full-order models that can be corrected easily. The d.c. gain difference may occur in cases where some parameters are eliminated without compensating their effects on the system. This is related to the various sensitivities of the system with respect to each of the parameters [14]. As an example, consider that the d.c. gain of the full-order model of a given system is $DC_{FM} = a_1 a_2$ and that $a_1 = 1, a_2 = 10$. If the model reduction leads to the elimination of $a_1 = 1$, then the d.c. gains of the full- and reduced-order models would be unchanged as $DC_{FM} = DC_{RM} = 10$. If the model reduction had led to the elimination of $a_2 = 10$, there would be a d.c. gain discrepancy of order 10 between $DC_{FM} = a_1 a_2 = 10$ and $DC_{RM} = a_1 = 1$. It should also be noted that if the output had been chosen as the flow variable, such as velocity, in a mechanical system that had a zero steady state value for a stable system then the reduced model would not have any d.c. gain error.

3 MODEL REDUCTION IMPLEMENTATIONS

In this section, a single-input, single-output (SISO) mechanical system, a hydraulic power system and a multi-input, multi-output (MIMO) mechanical system are used to illustrate the implementation of the physical model reduction and its interpretation.

3.1 A SISO system example

Consider the system shown in Fig. 11 and its bond graph representation shown in Fig. 12. The system is of order 4. However, the bond graph modelling method is considered to have five energy storage elements in integral causality. Hence, the system is of order 5 having one state in excess. The excess state is due to the structure of the system, since the spring k_2 does not generate an independent state. In this example the following values are chosen for the parameters: $m_1 = m_2 = 1$ kg,

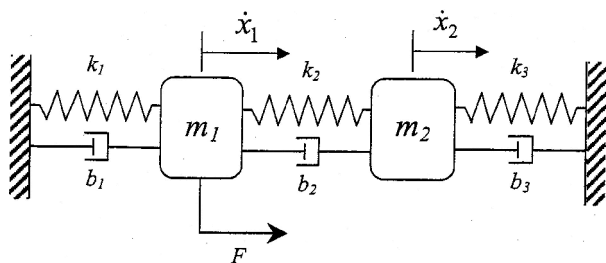


Fig. 11 An SISO physical system

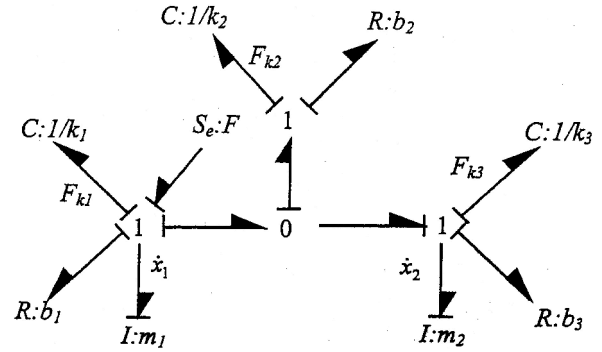


Fig. 12 Bond graph representation of the SISO physical system

$k_1 = k_3 = 1$ N/m, $k_2 = 15$ N/m, $b_1 = b_3 = 0.2$ N s/m, $b_2 = 1$ N s/m. Defining the power state variables, $x = [F_{k1} \ F_{k2} \ F_{k3} \ \dot{x}_1 \ \dot{x}_2]^T$, where F_{ki} , etc., represent the force in the i th spring, and $u = F$ as the input to the system, then the state-space equations become

$$\dot{x} = Ax + Bu \tag{1}$$

where the **A** and **B** matrices are given by

$$A = \begin{bmatrix} 0 & 0 & 0 & k_1 & 0 \\ 0 & 0 & 0 & k_2 & -k_2 \\ 0 & 0 & 0 & 0 & k_3 \\ -\frac{1}{m_1} & -\frac{1}{m_1} & 0 & -\frac{b_1 + b_2}{m_1} & \frac{b_2}{m_1} \\ 0 & \frac{1}{m_2} & -\frac{1}{m_2} & \frac{b_2}{m_2} & -\frac{b_2 + b_3}{m_2} \end{bmatrix} \tag{2}$$

$$B = \begin{bmatrix} 0 & 0 & 0 & \frac{1}{m_1} & 0 \end{bmatrix}^T \tag{3}$$

If the force F_{k1} is considered as the output variable then the output equation becomes

$$y = [1 \ 0 \ 0 \ 0 \ 0]x = Cx \tag{4}$$

The model reduction procedure is applied as follows:

Step 1: modelling. The bond graph model of the system is displayed in Fig. 12.

Step 2: decomposition. To perform the decomposition, the following local damping ratios and significant loop gains are calculated:

$$\frac{b_1}{2\sqrt{m_1 k_1}} = \frac{b_3}{2\sqrt{m_2 k_3}} = 0.1$$

$$\frac{b_2}{2\sqrt{m_1 k_2}} = \frac{b_2}{2\sqrt{m_2 k_2}} = 0.13$$

$$\frac{k_2}{m_1} = \frac{k_2}{m_2} = 15 \text{ rad/s}^2$$

and

$$\frac{k_1}{m_1} = \frac{k_3}{m_2} = 1 \text{ rad/s}^2$$

It is noted that the local damping ratios are fairly close to each other. Thus, it is not possible to immediately divide the system into two subsystems as a heavily damped and a lightly damped subsystem. However, it is possible to identify the high-frequency and low-frequency oscillation modes. The decomposition results in the two subsystems shown in Fig. 13.

Step 3: relevant modes. The calculated residues, their absolute values and the eigenvalues of the full-order system are shown in Table 2. The largest residue indicates the mode that contributes most to the dynamics of the system. Therefore, the eigenvalues that correspond to the bold-faced residues should be retained in the reduced model of order 2.

Step 4: matching modes to subsystems. The subsystems to be retained have now to be identified. To this end, the eigenvalues of subsystem 1 are computed as $\lambda_{1,2} = -0.1 \pm 0.9950i$ and the eigenvalues of subsystem 2 as $\lambda_{3,4} = -1 \pm 5.3852i$, $\lambda_5 = 0$, which are shown in Table 2. For a second-order reduced model, it is concluded that subsystem 1 should be retained and subsystem 2 should be eliminated. Therefore, subsystem 1 is selected as the reduced second-order model.

The time and frequency domain responses of the full-order and reduced-order models are compared in Figs 14 and 15. These plots indicate that the patterns are in good agreement. In Fig. 14 it is seen that the time domain responses have a very small absolute error of 0.0161 at steady state, which can be eliminated by a constant calibration factor. The frequency response plot shown in Fig. 15 shows that the mode at $\omega \cong 5.46$ rad/s is eliminated from the two-mode full-order model, which justifies the proposed model reduction method.

3.2 Hydraulic line of a power steering system

In this section, the model reduction will be applied to a linearized hydraulic line of a power steering system,

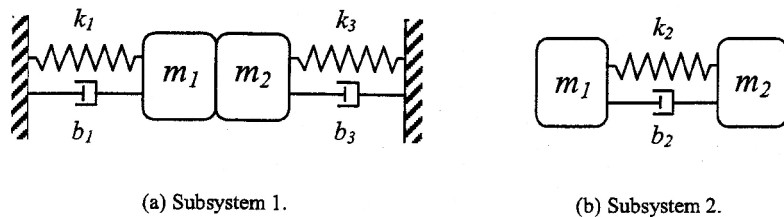


Fig. 13 Subsystems of the SISO physical system

Table 2 Residues, their absolute values and eigenvalues of the SISO system

Original system			Subsystem
Residues	Absolute values	Eigenvalues	Eigenvalues
$-0.0000 \mp 0.2513i$	0.2513	$-0.1000 \pm 0.9950i$	$-0.1000 \pm 0.9950i$
$-0.0000 \mp 0.0458i$	0.0458	$-1.1000 \pm 5.4580i$	$-1.1 \pm 5.3852i, 0.0000$
0.0000	0.0000	0.0000	

shown schematically in Fig. 16 [11, 15]. The hydraulic line is assumed to be open to air at the valve end. The effective resistance of the rotary valve indicated by R_V will thus be zero ($R_V = 0$ N s/m⁵). The parameter values for the pipes and the hoses are tabulated in Tables 3 and 4.

Choosing the state vector as

$$x = [P_P \ Q_{P1} \ P_{H1} \ Q_{P2} \ P_{H2} \ Q_{P3}]^T$$

where P_P , Q_{Pi} and P_{Hi} stand for the pressure at the pump outlet port, the flowrate through pipe i and the pressure in hose i respectively, the state-space equations can be written as

$$\dot{x} = Ax + Bu \tag{5}$$

where the **A** and **B** matrices are given by

$$A = \begin{bmatrix} 0 & -\frac{1}{C_{P1}} & 0 & 0 & 0 & 0 \\ \frac{1}{I_{P1}} & -\frac{R_{P1}}{I_{P1}} & -\frac{1}{I_{P1}} & 0 & 0 & 0 \\ 0 & \frac{1}{C_{H1}} & 0 & -\frac{1}{C_{H1}} & 0 & 0 \\ 0 & 0 & \frac{1}{I_{P2}} & -\frac{R_{P2}}{I_{P2}} & -\frac{1}{I_{P2}} & 0 \\ 0 & 0 & 0 & \frac{1}{C_{H2}} & 0 & -\frac{1}{C_{H2}} \\ 0 & 0 & 0 & 0 & \frac{1}{I_{P3}} & -\frac{R_{P3} + R_V}{I_{P3}} \end{bmatrix} \tag{6}$$

$$B = \begin{bmatrix} \frac{1}{C_{P1}} & 0 & 0 & 0 & 0 & 0 \end{bmatrix}^T \tag{7}$$

Assuming that the output state variable is the pressure

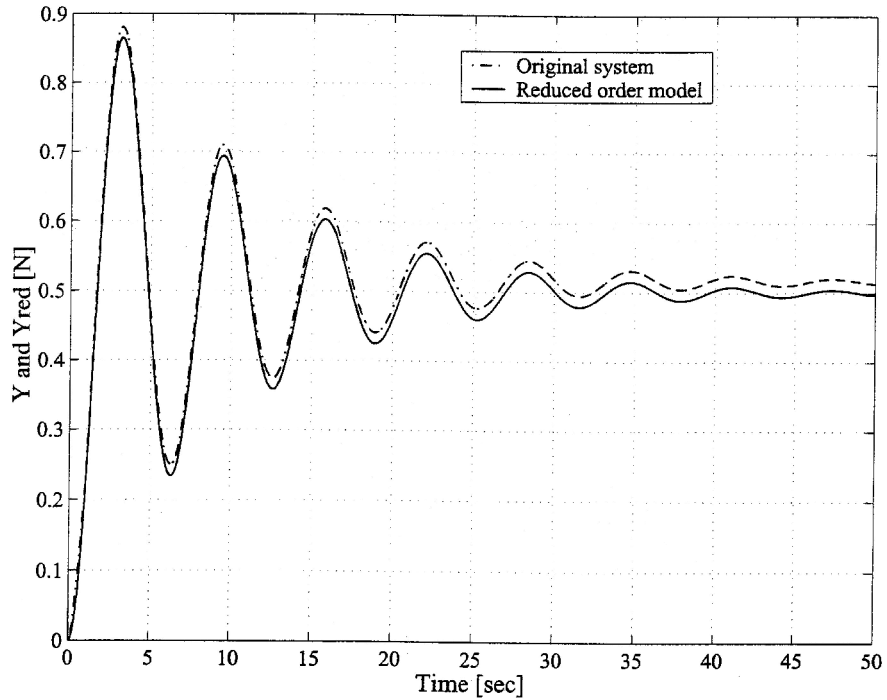


Fig. 14 Comparison of step responses using subsystem 1

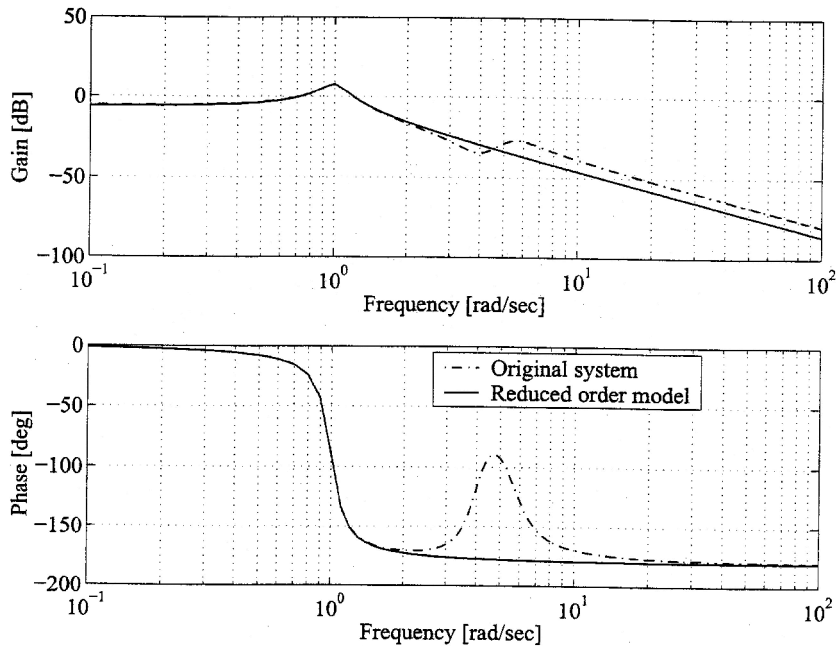


Fig. 15 Comparison of frequency responses using subsystem 1

P_p , then the output equation can be written as

$$y = P_p = [1 \ 0 \ 0 \ 0 \ 0 \ 0]x = Cx \quad (8)$$

The hydraulic line is of order 6. In order to decompose this system into its subsystems, the following loop gains can be calculated:

$$\frac{1}{I_{P1} C_{P1}} = 102.63 \times 10^6 \text{ rad/s}^2$$

$$\frac{1}{I_{P1} C_{H1}} = 0.41 \times 10^6 \text{ rad/s}^2$$

$$\frac{1}{I_{P2} C_{H1}} = 0.16 \times 10^6 \text{ rad/s}^2$$

$$\frac{1}{I_{P2} C_{H2}} = 0.32 \times 10^6 \text{ rad/s}^2$$

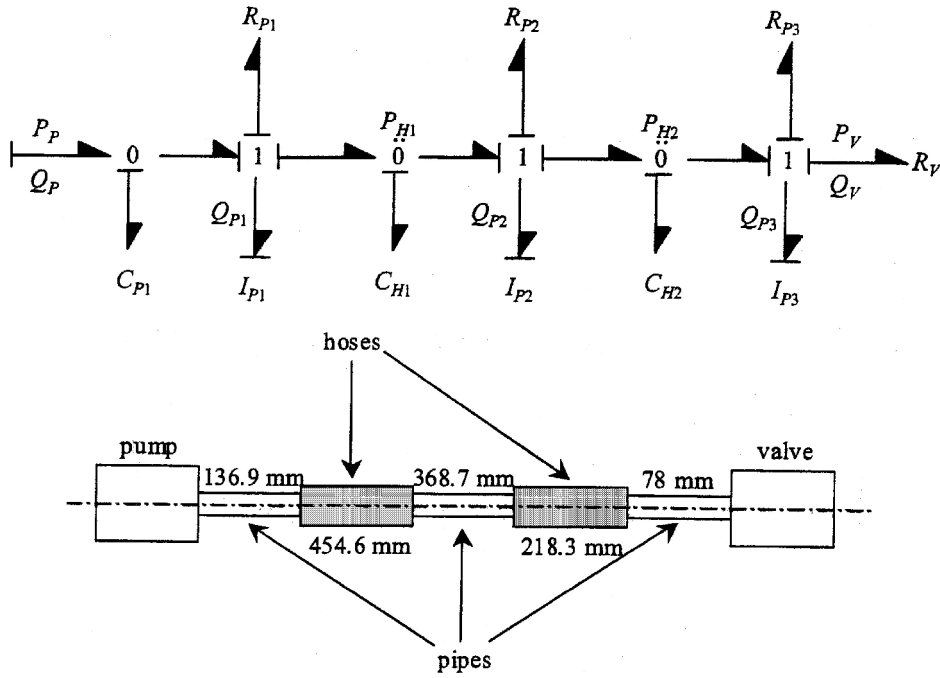


Fig. 16 Schematic and bond graph representation of a hydraulic line

Table 3 Parameter values for pipes

Pipe number	L_p (m)	I_p (kg/m ⁴)	R_p (N s/m ⁵)	C_p (m ⁵ /N)
1	1.369×10^{-1}	1.45×10^6	5.30×10^6	6.72×10^{-15}
2	3.687×10^{-1}	3.90×10^6	1.43×10^7	1.81×10^{-14}
3	7.8×10^{-2}	8.24×10^5	3.02×10^6	3.83×10^{-15}

Table 4 Parameter values for hoses

Hose number	L_H (m)	C_H (m ⁵ /N)
1	4.546×10^{-1}	1.67×10^{-12}
2	2.183×10^{-1}	8.0×10^{-13}

$$\frac{1}{I_{P3} C_{H2}} = 1.52 \times 10^6 \text{ rad/s}^2$$

The local damping ratios are calculated as

$$\frac{R_{P1}}{2\sqrt{I_{P1}/C_{P1}}} = 1.80 \times 10^{-4}$$

$$\frac{R_{P1}}{2\sqrt{I_{P1}/C_{H1}}} = 2.84 \times 10^{-3}$$

$$\frac{R_{P2}}{2\sqrt{I_{P2}/C_{H1}}} = 4.68 \times 10^{-3}$$

$$\frac{R_{P2}}{2\sqrt{I_{P2}/C_{H2}}} = 4.87 \times 10^{-4}$$

$$\frac{R_{P3}}{2\sqrt{I_{P2}/C_{H2}}} = 6.84 \times 10^{-4}$$

$$\frac{R_{P3}}{2\sqrt{I_{P3}/C_{H2}}} = 1.49 \times 10^{-3}$$

Application of the decomposition procedures suggests that the hydraulic line can be separated into three subsystems. The first subsystem consists of I_{P1} , C_{P1} and R_{P1} (a second-order system), the second and the third subsystems consist of I_{P2} , C_{H1} , R_{P2} , and I_{P3} , C_{H2} , R_{P3} . The eigenvalues of these subsystems are tabulated in Table 5. In addition, the residues, absolute values of the residues and the corresponding eigenvalues of the original system are tabulated in Table 5. It is seen that the first mode is the most important one and it should be retained in a reduced-order model. Thus, the hydraulic line can be reduced from order 6 to order 2 by using the first subsystem as the reduced-order model. The time and frequency responses of this system for a step input of $Q_p = 1 \times 10^{-4} \text{ m}^3/\text{s}$ are displayed in Fig. 17. It is seen that the first resonance frequency of the full model disappears as a result of being reduced to a second-order model. A small d.c. gain difference exists in the magnitude plots that can be corrected by a constant factor.

3.3 A MIMO system example

As a third illustrative example, the method is applied to the MIMO system of Fig. 18 whose bond graph is shown in Fig. 19. This system has seven independent energy storage elements in integral causality; thus it is of order seven.

Using the power state variables ($\dot{x}_4, F_{k3}, \dot{x}_3, F_{k2}, \dot{x}_2, F_{k1}, \dot{x}_1$), where F_{k_i} represents the force in spring i and F_1 and F_2 are two inputs respectively, the following state-space representation is obtained:

$$\dot{x} = Ax + Bu \tag{9}$$

where the **A** and **B** matrices are given by

Table 5 Residues, their absolute values and the corresponding eigenvalues of the hydraulic line

Original system			Subsystem
Residues	Absolute values	Eigenvalues	Eigenvalues
$7.41 \times 10^{13} \mp 1.33 \times 10^{10}i$	7.41×10^{13}	$-1.83 \pm 10151i$	$-1.83 \pm 10130i$
$2.94 \times 10^{11} \mp 1.53 \times 10^9i$	2.94×10^{11}	$-1.83 \pm 352.74i$	$-1.83 \pm 392.03i$
$5.09 \times 10^9 \mp 6.8 \times 10^6i$	5.08×10^9	$-1.83 \pm 1366.1i$	$-1.83 \pm 1231.7i$

$$\mathbf{A} = \begin{bmatrix} -\frac{b_3}{m_4} & \frac{1}{m_4} & \frac{b_3}{m_4} & 0 & 0 & 0 & 0 \\ -k_3 & 0 & k_3 & 0 & 0 & 0 & 0 \\ \frac{b_3}{m_3} & -\frac{1}{m_3} & -\frac{b_2+b_3}{m_3} & \frac{1}{m_3} & \frac{b_2}{m_3} & 0 & 0 \\ 0 & 0 & -k_2 & 0 & k_2 & 0 & 0 \\ 0 & 0 & \frac{b_2}{m_2} & -\frac{1}{m_2} & -\frac{b_1+b_2}{m_2} & \frac{1}{m_2} & \frac{b_1}{m_2} \\ 0 & 0 & 0 & 0 & -k_1 & 0 & k_1 \\ 0 & 0 & 0 & 0 & \frac{b_1}{m_1} & -\frac{1}{m_1} & -\frac{b_1}{m_1} \end{bmatrix}, \quad \mathbf{B} = \begin{bmatrix} 0 & \frac{1}{m_4} \\ 0 & 0 \\ 0 & 0 \\ 0 & 0 \\ 0 & 0 \\ \frac{1}{m_1} & 0 \end{bmatrix}$$

Assuming the velocities \dot{x}_1 and \dot{x}_2 of masses m_1 and m_2 are of interest, the output vector equation is given by

$$\mathbf{y} = \mathbf{C}\mathbf{x} \quad (10)$$

where \mathbf{C} is

$$\mathbf{C} = \begin{bmatrix} 0 & 0 & 0 & 0 & 0 & 0 & 1 \\ 0 & 0 & 0 & 0 & 1 & 0 & 0 \end{bmatrix}$$

The subsystems shown in Fig. 20 are obtained using the decomposition procedure described earlier. Assuming that $m_1 = m_2 = m_3 = m_4 = 1$ kg, $k_1 = 4$ N/m, $k_2 = 2$ N/m, $k_3 = 8$ N/m, $b_1 = 1$ N s/m, $b_2 = 2$ N s/m and $b_3 = 4$ N s/m, the necessary loop gains and local damping ratios are calculated as

$$\frac{k_1}{m_1} = \frac{k_1}{m_2} = 4 \text{ rad/s}^2, \quad \frac{k_2}{m_2} = \frac{k_2}{m_3} = 2 \text{ rad/s}^2$$

$$\frac{k_3}{m_3} = \frac{k_3}{m_4} = 8 \text{ N s/m}$$

$$\frac{b_1}{2\sqrt{k_1 m_1}} = \frac{b_1}{2\sqrt{k_1 m_2}} = 0.25$$

$$\frac{b_2}{2\sqrt{k_2 m_2}} = \frac{b_2}{2\sqrt{k_2 m_3}} = 0.707$$

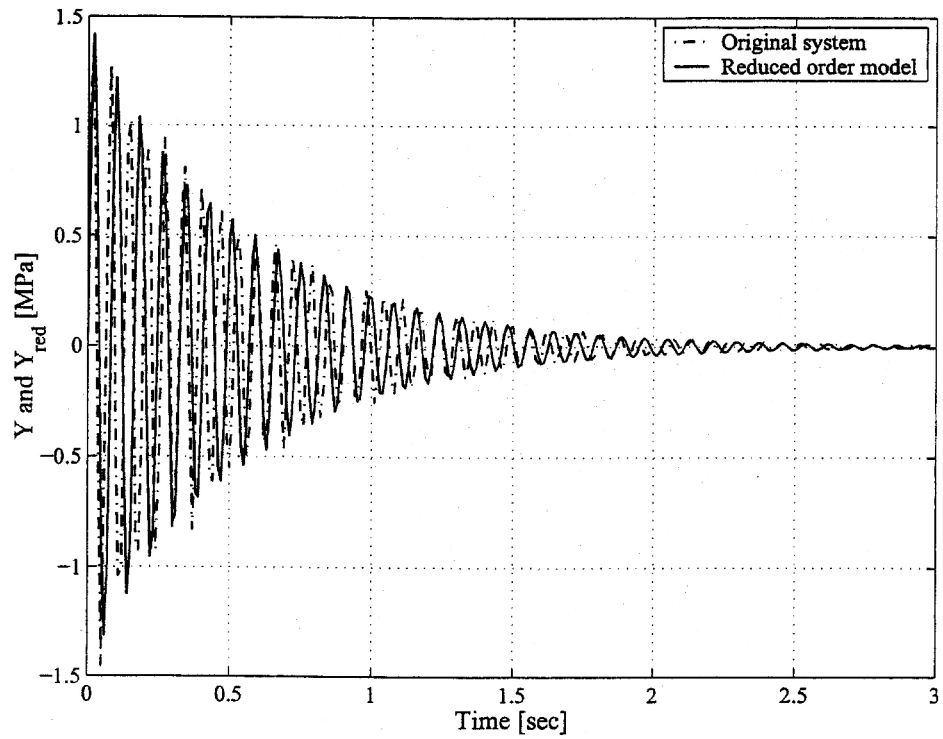
$$\frac{b_3}{2\sqrt{k_3 m_3}} = \frac{b_3}{2\sqrt{k_3 m_4}} = 0.707$$

Subsystems 4 and 5 are obtained from subsystem 1. The eigenvalues of the subsystems are shown in Table 6. The eigenvalues of the overall system, their corresponding

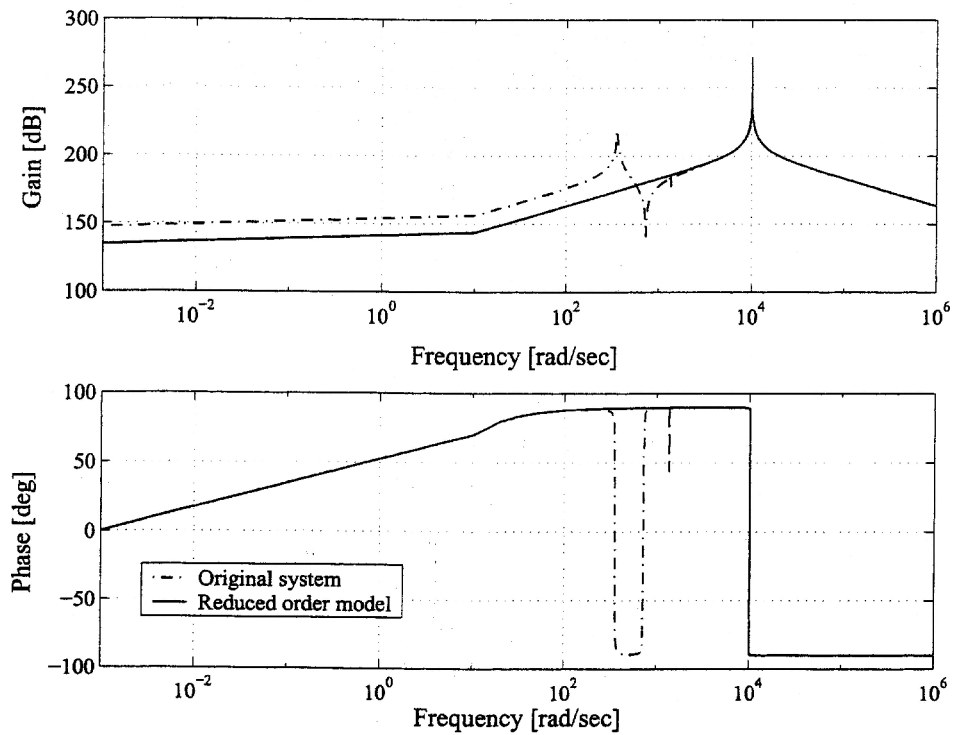
residues and the 2-norms are listed in Table 7. Notice that any norm could have been used in the model reduction process. The norms of the residues suggest that the eigenvalues corresponding to the bold-faced residues in Table 7 should be retained in the reduced-order model. The analysis shows that the subsystem 1 is the dominant one. Thus, the first subsystem is chosen as the reduced-order model. The time and frequency responses of the overall system and its reduced-order model are displayed in Figs 21 and 22 respectively. These results show that there is a good agreement between the full- and the reduced-order models in the MIMO case as well.

4 CONCLUSIONS

In this paper a model reduction procedure that uses information from the physical domain is presented. The proposed methodology exploits the idea of decomposition of physical systems suitable for the identification of dominant subsystems. Most of the previous model reduction techniques use numerical approaches and the resulting reduced-order model does not have a physical relevance to the original system. Physical-based model reduction methods making use of bond graphs and power and energy level information eliminate elements that are considered unnecessary without indicating which subsystems to remove in a systemic perspective view. In contrast, the proposed decomposition and model reduction procedures are directly implemented on



(a) Comparison of time responses.



(b) Comparison of frequency responses.

Fig. 17 Comparison of responses of the hydraulic line

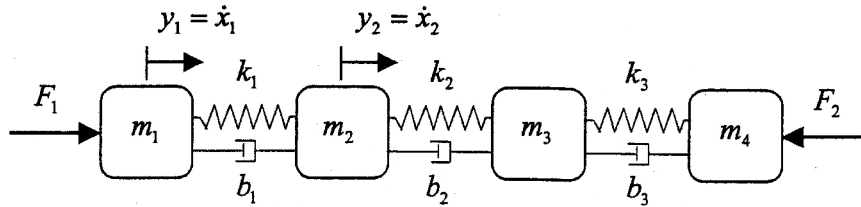


Fig. 18 A seventh-order MIMO physical system

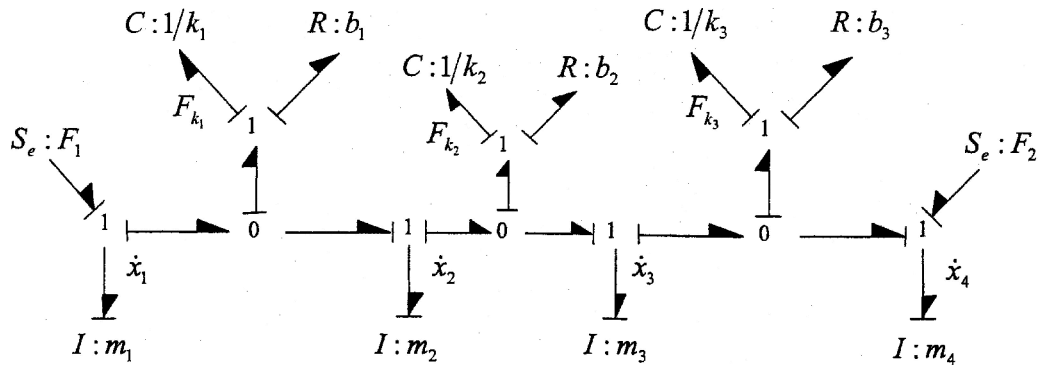


Fig. 19 Bond graph representation of the seventh-order MIMO physical system

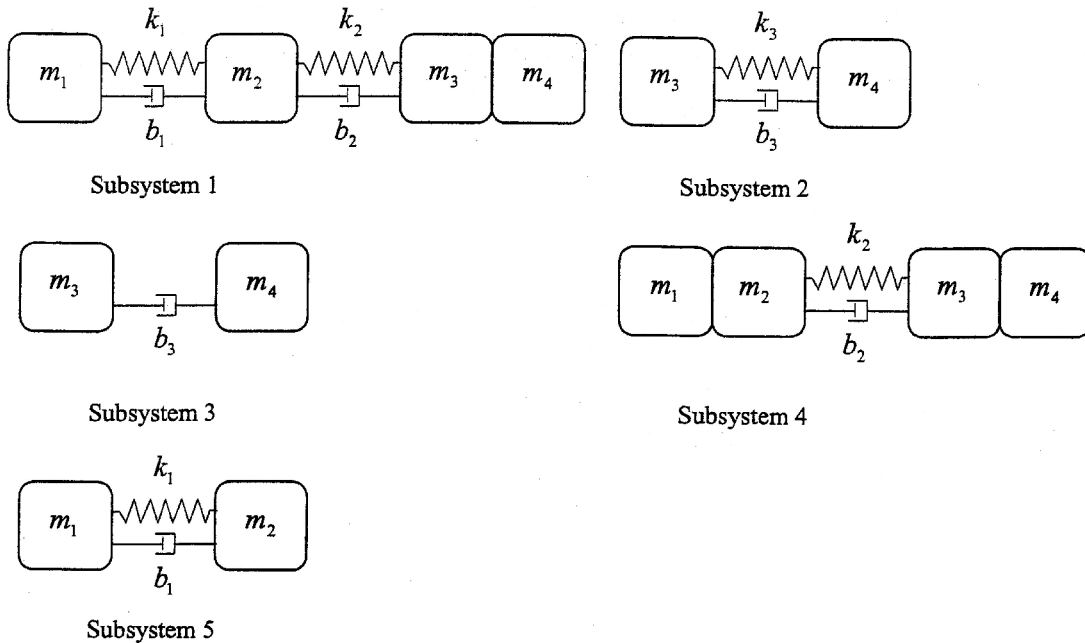


Fig. 20 Subsystems of the seventh-order MIMO physical system

the model, providing a better perception of the physical model reduction and a better design point of view. In addition to this feature, the method of Sueur and Dauphin–Tanguy is improved using the extended decomposition procedures to identify: (a) fast–slow dynamics, (b) high–low-frequency oscillation modes and

(c) heavily–lightly damped dynamic subsystems. The additional use of type (b) and type (c) dynamic subsystems in conjunction with the residues and eigenvalues information for model reduction constitutes the main contribution of the present approach. The relevant physical subsystems are retained by assessing the

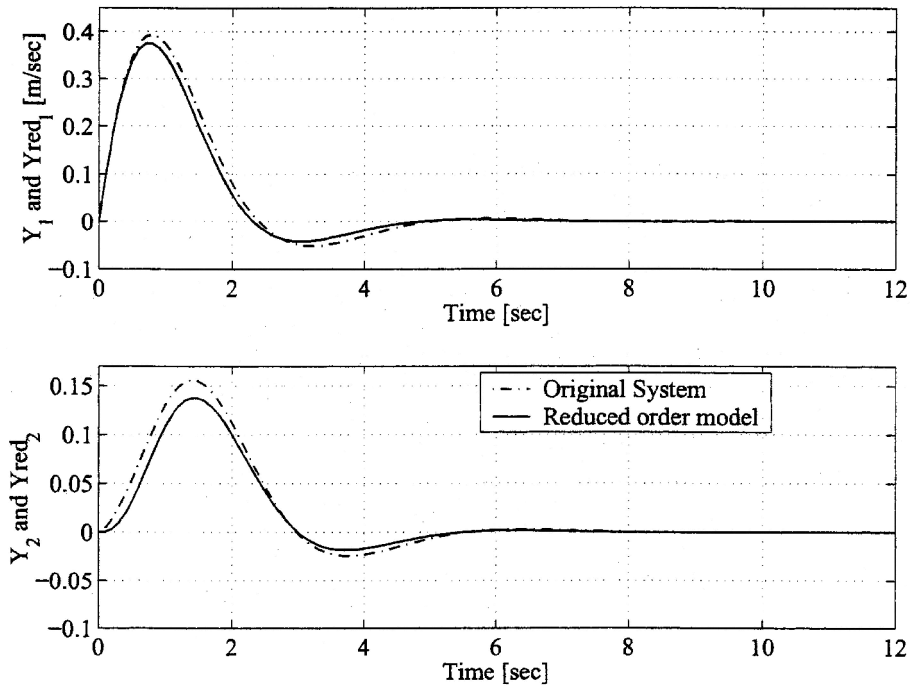


Fig. 21 Comparison of step responses

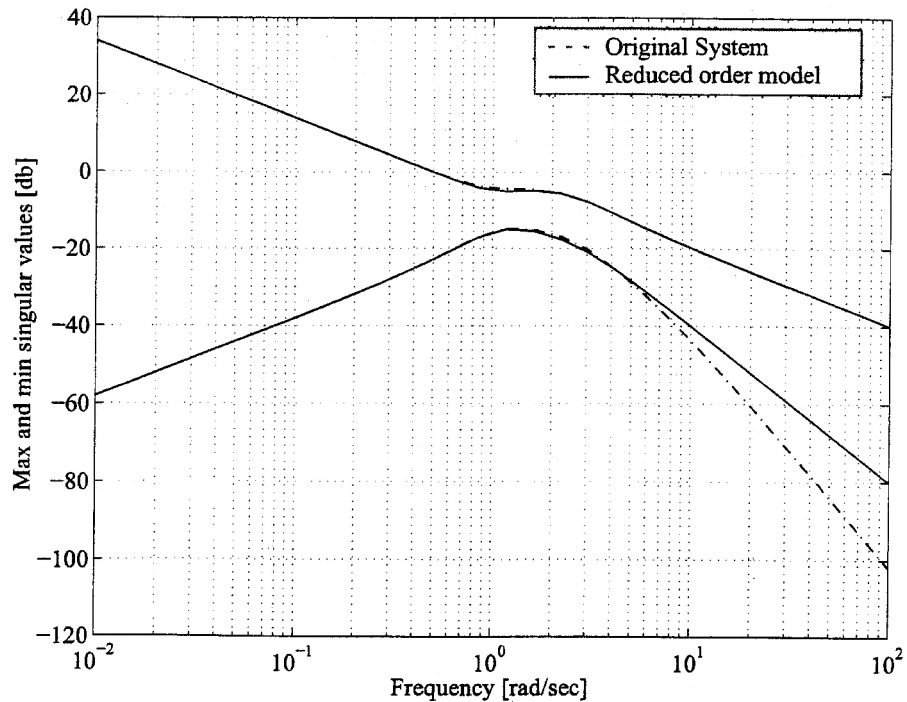


Fig. 22 Comparison of frequency responses

absolute values of the residues of the full model. The physical model reduction procedure is verified on three linear physical system examples. The reduced-order model responses were found to be in good agreement

with their full-order counterparts, except for slight discrepancies in steady state values due to a natural result of the model reduction process, which may be corrected by a constant gain factor.

Table 6 Eigenvalues of the subsystems of the seventh-order MIMO system

Eigenvalue	Subsystem
$-0.0000 \mp 0.0458i$	1
$-0.9225 \pm 1.2199i$	1
0	1
-4	2
-4	2
-8	3
$-1.0000 \pm 1.0000i$	4
$-1.0000 \pm 2.6458i$	5

Table 7 Residues, their 2-norms and the eigenvalues of the seventh-order MIMO system

Residue	2-norm	Eigenvalue
$\begin{bmatrix} 0.001 & -0.0150 \\ -0.008 & 0.2220 \end{bmatrix}$	0.2229	-7.1429
$\begin{bmatrix} 0.197 \mp 0.093i & 0.107 \pm 0.126i \\ -0.304 \mp 0.076i & -0.005 \mp 0.238i \end{bmatrix}$	0.4792	$-1.5381 \pm 2.3328i$
$\begin{bmatrix} 0.185 \pm 0.231i & -0.217 \mp 0.179i \\ 0.2082 \pm 0.052i & -0.204 \mp 0.007i \end{bmatrix}$	0.5049	$-0.7959 \pm 1.2097i$
$\begin{bmatrix} 0.25 & 0.25 \\ 0.25 & 0.25 \end{bmatrix}$	0.5	0
$\begin{bmatrix} -0.014 & -0.015 \\ -0.051 & -0.055 \end{bmatrix}$	0.0778	-2.1888

REFERENCES

- Moore, B. C.** Principal component analysis in linear systems: controllability, observability, and model reduction. *IEEE Trans. Autom. Control*, 1981, **26**(1), 17–32.
- Davidson, A. M.** and **Walters, I. R.** Linear system reduction using approximate moment matching. *IEE Proc., Part D*, 1988, **135**(2), 73–78.
- Lalonde, R. J., Hartley, T. T.** and **De Abreu-Garcia, J. A.** Least squares model reduction. *J. Franklin Inst.*, 1992, **329**(2), 215–240.
- Skelton, R. E.** and **Yousuff, A.** Component cost analysis of large-scale systems. *Int. J. Control*, 1983, **37**(2), 285–304.
- Xiheng, H.** FF-Padé method of model reduction in frequency domain. *IEEE Trans. Autom. Control*, March 1987, **32**(3), 243–246.
- Shieh, L. S.** and **Gaudino, F. F.** Matrix continued fraction expansion and inversion by the generalized matrix Routh algorithm. *Int. J. Control*, 1974, **20**(5), 727–737.
- Safonov, M. G.** and **Chiang, R. Y.** A Schur method for balanced-truncation model reduction. *IEEE Trans. Autom. Control*, July 1989, **34**(7), 729–733.
- Rosenberg, R. C.** and **Zhou, T.** Power based model insight. In Proceedings of the 1988 ASME Winter Annual Meeting on *Automated Modeling for Design*, Chicago, Illinois, 27 November–2 December 1988, The Dynamic Systems and Controls Division, pp. 61–67.
- Louca, L. S., Stein, J. L., Hulbert, G. M.** and **Sprague, J.** Proper model generation: an energy-based methodology. In Proceedings of the 3rd International Conference on *Bond Graph Modeling (ICBGM'97)*, Phoenix, Arizona, January 1997, Vol. 29, No. 1, pp. 44–49 (SCS, The Society for Modeling and Simulation International, San Diego, California).
- Sueur, C.** and **Dauphin-Tanguy, G.** Bond graph approach for multi-time scale system analysis. *J. Franklin Inst.*, 1991, **328**(5), 1005–1026.
- Orbak, A. Y.** Physical domain model reduction for design and control of engineering systems. MechE thesis, Mechanical Engineering Department, Massachusetts Institute of Technology, Cambridge, Massachusetts, June 1998.
- Huang, S.-Y.** Structural analysis from system configurations for modeling and design of multi-energy domain dynamic systems. PhD dissertation, Mechanical Engineering Department, Massachusetts Institute of Technology, Cambridge, Massachusetts, June 1997.
- Huang, S.-Y.** and **Youcef-Toumi, K.** Structural analysis for modeling and design of multi-energy domain dynamic systems. In Proceedings of the IEEE/ASME International Conference on *Advanced Intelligent Mechatronics (AIM97)*, Tokyo, Japan, June 1997, pp. 155–160.
- Burrows, C. R.** and **Turkay, O. S.** A sensitivity analysis of squeeze-film bearings. *Trans. ASME, J. Lubric. Technol.*, 1982, **104**, 516–522.
- Orbak, A. Y., Youcef-Toumi, K.** and **Senga, M.** Model reduction and design of a power steering system. In Proceedings of the American Control Conference (ACC99), San Diego, California, 1999, pp. 4476–4481.

Copyright of Proceedings of the Institution of Mechanical Engineers -- Part I -- Journal of Systems & Control Engineering is the property of Professional Engineering Publishing and its content may not be copied or emailed to multiple sites or posted to a listserv without the copyright holder's express written permission. However, users may print, download, or email articles for individual use.